

# Transmission electron microscopy, x-ray diffraction and Raman scattering studies of nanophase TiO<sub>2</sub>

---

Turković, Aleksandra; Tonejc, Anđelka; Popović, Stanko; Dubček, Pavo; Ivanda, Mile; Musić, Svetozar; Gotić, Marijan

Source / Izvornik: **Fizika A, 1997, 6, 77 - 88**

Journal article, Published version

Rad u časopisu, Objavljena verzija rada (izdavačev PDF)

Permanent link / Trajna poveznica: <https://um.nsk.hr/um:nbn:hr:217:973082>

Rights / Prava: [In copyright](#)/[Zaštićeno autorskim pravom.](#)

Download date / Datum preuzimanja: **2024-11-20**



Repository / Repozitorij:

[Repository of the Faculty of Science - University of Zagreb](#)



TRANSMISSION ELECTRON MICROSCOPY, X-RAY DIFFRACTION AND  
RAMAN SCATTERING STUDIES OF NANOPHASE TiO<sub>2</sub>  
(A review paper)

ALEKSANDRA TURKOVIĆ<sup>a</sup>, ANĐELKA TONEJC<sup>b</sup>, STANKO POPOVIĆ<sup>a,b</sup>, PAVO  
DUBČEK<sup>a</sup>, MILE IVANDA<sup>a</sup>, SVETOZAR MUSIĆ<sup>a</sup> and MARIJAN GOTIĆ<sup>a</sup>

<sup>a</sup>*Rudjer Bošković Institute, P. O. Box 1016, 10001 Zagreb, Croatia*

<sup>b</sup>*Department of Physics, Faculty of Sciences, University of Zagreb, P. O. Box 162, 10001 Zagreb, Croatia*

Received 17 January 1997

Revised manuscript received 27 March 1997

UDC 538.975

PACS 68.55.Nq, 81.15.Lm

**This paper is dedicated to Professor A. Bonefačić on the occasion  
of his 70<sup>th</sup> birthday**

Dye-sensitized solar cells differ from conventional semiconductor devices in that they separate the function of light absorption from charge-carrier transport. The device is based on a 10- $\mu\text{m}$ -thick optically transparent film of titanium dioxide (TiO<sub>2</sub>) particles of a few nanometers in size, coated with a monolayer of charge-transfer dye to sensitize the film for light harvesting. In the present authors' review, the principal role of the TiO<sub>2</sub> photoanode is emphasized by a detailed presentation of its characterization by different experimental methods, while the photoelectric responses of the cells, a work which is still in progress, are indicated in the references cited. Hydrolysis of Ti(IV)-isopropoxide in isopropanol by the addition of water is a suitable chemical reaction for the production of nanosized TiO<sub>2</sub>. The properties of nanosized TiO<sub>2</sub> can be modified by the hydrolysis catalyst, pH of the solution, temperature, presence of complexing ligand and the colloidal state of TiO<sub>2</sub> precursor. In the present work, the microstructural properties of nanosized TiO<sub>2</sub> were studied by HREM, ED, XRD, SAXS and Raman spectroscopy. HREM was used to determine

both grain and pore sizes. Electron diffraction and X-ray diffraction provided evidence of nanocrystalline anatase and brookite phases. The grain sizes of the anatase and brookite phases changed from  $(5 \pm 1)$  to  $(12 \pm 3)$  nm with an increase of the treating temperature up to 773 K, as shown by XRD. An method of determining nanosized TiO<sub>2</sub> grain size based on low-frequency Raman scattering, is presented.

## 1. Introduction

Titanium dioxide particles of very small dimensions have important applications in photovoltaic devices. For example, TiO<sub>2</sub> thin films, obtained by chemical vapour deposition (CVD) [1] or spray technique [2], have been utilized as intercalation electrodes for Ag/AgI/ TiO<sub>2</sub>, SnO<sub>2</sub> rechargeable and photosensitive galvanic cells [2]. The Ag<sup>+</sup> ion diffusion in TiO<sub>2</sub> and thus the kinetics of the electrochemical intercalation reaction are greatly influenced by the properties of the oxide electrode. In order to achieve a better understanding of the role of TiO<sub>2</sub> in these cells, various characterizations of TiO<sub>2</sub> thin films were performed using X-ray diffraction, Raman spectroscopy, thermally stimulated currents (TSC), photoresistance wavelength dependence in the range from 250 to 350 nm, FT-IR spectroscopy, X-ray photoelectron spectroscopy (XPS) and UV-Vis absorption [3–9].

In the last twenty years, a considerable scientific and engineering effort has been focused on the development of photovoltaic solar cells [10]. Excellent results have been achieved in the development of different types. Although these solar cells were technically very satisfactory, they were not competitive against the price of electricity generated in standard electrical power plants.

In 1991, Grätzel and his research group made a breakthrough in preparing an efficient dye-sensitized cell utilizing a relatively non-pure raw material and an inexpensive preparation procedure [11]. Energy conversion efficiencies from 7 to 12% were achieved. All previous attempts to produce a stable electrochemical cell from semiconductors with an adequate energy gap for solar light absorption had failed because of the photocorrosion effect. Photo-generated minor charge-carriers at the semiconductor electrolyte boundary act as oxidants and destroy the photoanode. The new type of solar cell mimics the natural process of photosynthesis, and it is even more efficient in energy conversion than the traditional solar cells. It differs from the conventional semiconductor device in that it separates the function of light absorption from that of charge-carrier transport. For us, it was a great satisfaction to learn that TiO<sub>2</sub> semiconductor electrodes were used in these solar cells, as we used the same material in the photosensitive galvanic cells [2,3]. In our cell, the application of the AgI-TiO<sub>2</sub> system produced a shift of the absorption maximum to the visible region of the solar spectrum. This shift was not significant as in the case of dye-coated TiO<sub>2</sub> thin films [11], but the idea of moving the absorption edge of TiO<sub>2</sub> (anatase, with a band gap of 3.2 eV) to the visible region, in order to obtain efficient solar cells or photo-batteries, was essentially the same. In the work by O'Regan and Grätzel [11], TiO<sub>2</sub> thin films were prepared using sol-gel procedure. The high surface area of TiO<sub>2</sub> semiconductor electrodes was sensitized with different Ru(bpy)-complexes. Light-to-electric energy conversion efficiencies of 10% in simulated solar light (AM 1.5)[11] and 12% in diffuse

daylight [12] were reported. The long time stability of the above-mentioned solar-cells was reported, sustaining at least  $10^7$  turnovers, the longest reported continuous exposure time being 10 months.

In order to improve the properties of the Grätzel cell, scientists and engineers have focused their research and development on the components of this solar cell, such as  $\text{TiO}_2$ , electrolyte solution and dye. We also investigated [3-9,13]  $\text{TiO}_2$  from different standpoints using various techniques, such as X-ray diffraction, electron diffraction, TEM, HREM and DTA.

In the present review, we shall present and discuss selected results of the microstructural characterization of nanosized  $\text{TiO}_2$ , as obtained in our previous investigations.  $\text{TiO}_2$  was prepared using sol-gel procedure. The optimization of sol-gel procedure for  $\text{TiO}_2$  preparation was also investigated. The aim of this research was to obtain nanosized  $\text{TiO}_2$  with improved properties, which could be useful for its application as photoanode in dye-sensitized solar cells, as well as in electrochromic devices.

## 2. Experimental

Chemicals supplied by Aldrich and Merck were used. Water was doubly distilled. The precipitation of  $\text{TiO}_2$  precursor was performed by hydrolysis of Ti(IV)-isopropoxide in a specially designed glass apparatus. The experimental procedures of the preparation of the samples are described in previous publications [14-18].

The  $\text{TiO}_2$  samples were examined by transmission electron microscopy (TEM), including bright-field (BF) and dark-field (DF) microscopy, electron diffraction (ED) and high resolution electron microscopy (HREM). TEM and HREM investigations were performed with the JEOL JEM 2010 200 keV electron microscope, having  $C_s = 0.5$  mm and point resolution of 0.19 nm.

X-ray powder diffraction measurements were performed at room temperature using a Philips counter diffractometer (MPD 1880) with monochromatized  $\text{CuK}\alpha$  radiation.

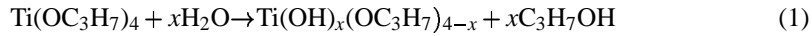
Small angle X-ray scattering (SAXS) is a powerful experimental technique in determining the grain or pore shape and size in the range from 1 to 100 nm. A drawback in its application on thin films is the presence of a substrate which usually substantially reduces the primary beam intensity. SAXS measurements were performed using a standard Kratky camera.

Raman spectra were recorded using a Dilor Z-24 Raman spectrometer in the back scattering configuration, using 50 mW of focused 514.5 nm argon laser excitation.

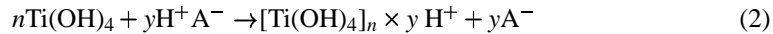
## 3. Results and discussion

### 3.1. General view of nanosized $\text{TiO}_2$ obtained by sol-gel procedure

The hydrolysis of Ti(IV)-isopropoxide with water in isopropanol, can be described by the following equation



If there is an excess of water, the hydroxide phase, which may also include the Ti(IV)-hydroxy polymers, is completely precipitated. The  $\text{Ti}(\text{OH})_4$  aggregates can be peptized into stable colloids by acidification of the suspension with HCl or  $\text{HNO}_3$ . Adsorption of  $\text{H}^+$  ions onto the surface of  $\text{Ti}(\text{OH})_4$  aggregates gives the positive charge to colloidal particles, so these particles exist in a stabilized state. The process of adsorption of  $\text{H}^+$  ions onto the surface of  $\text{Ti}(\text{OH})_4$  aggregates can be written as



Peptization is a temperature dependent process. The phase composition of the products of aging of the  $\text{TiO}_2$  precursor in aqueous medium depends on the colloidal state (polymer, sol, gel, precipitate) and other factors. Additional stabilization of  $\text{TiO}_2$  colloids can be achieved by the addition of polymers, for example HPC (hydroxypropyl cellulose), PEG (polyethylene glycol), etc. These polymers also prevent sintering of particles during the calcination of the  $\text{TiO}_2$  precursor. Before reviewing our results, we shall first focus our attention on selected achievements of other researchers in the field of  $\text{TiO}_2$  synthesis from Ti(IV)-alkoxide.

Papoutsis and Lianos [19,20] used water in-oil (W/O) microemulsions to produce  $\text{TiO}_2$  gel suitable for thin film preparation. Ti(IV)-isopropoxide was the starting material in the synthesis of  $\text{TiO}_2$  gel. Courtecuisse et al. [21] also used Ti(IV)-isopropoxide in the synthesis of fine  $\text{TiO}_2$  powders; however, the synthesis was performed in supercritical isopropyl alcohol.  $\text{TiO}_2$  photocatalysts (aerogels) were prepared [22] using hydrolysis of Ti(IV)-isopropoxide and supercritical point drying. The porosity of these aerogels measured by BET was 85% and the surface area was  $600 \text{ m}^2/\text{g}$ . These aerogels have a bulk density of  $0.5 \text{ g/cm}^3$ . X-ray diffraction showed the existence of anatase phase with a crystallite size of 5 nm. Nishide and Mizukami [23] investigated formation of  $\text{TiO}_2$  by hydrolysis of Ti(IV)-isopropoxide in the presence of various complexing ligands. The presence of complexing ligands influenced the size of  $\text{TiO}_2$  particles, crystal phases and refractive indices of  $\text{TiO}_2$  films on glass substrates. Nagpal et al. [24] prepared  $\text{TiO}_2$  thin films on quartz or silicon substrates using  $\text{TiO}_2$  colloid dispersion stabilized with HPC polymer. The  $\text{TiO}_2/\text{HPC}$  composite films were transparent in the visible region and completely blocked UV radiation at 300 nm. Transparent films of amorphous  $\text{TiO}_2$  were made by burning out the HPC at  $500^\circ \text{C}$ .

The mechanism of polycondensation of Ti(IV)-isopropoxide with orthoboric acid in pyridine at  $60^\circ \text{C}$  has been studied [25] by  $^1\text{H}$  and  $^{13}\text{C}$  nuclear magnetic resonance (NMR). The degree of polymerization and the nature of the hydrolytic species formed in the reaction were determined by the boric acid/alkoxide ratio. Transfer of the alkyl groups from alkoxide to boric acid is monitored spectroscopically. Lopez et al. [26] characterized  $\text{TiO}_2$ , prepared by sol-gel procedure, using FT-IR and UV-Vis (diffuse reflectance) spectroscopies. Correlations were found between the formation of  $\text{TiO}_2$  polymorph (anatase or rutile) and catalyst of hydrolysis reaction, pH and calcination temperature.

The porous texture of  $\text{TiO}_2$  gel produced from Ti(IV)-isopropoxide was investigated [27] using small angle X-ray scattering (SAXS) and thermoporometry. In decane, a pore radius of 2 to 2.8 nm was measured, while the hydrolysis of residual organic groups in the

gel, with prolonged aging in water, gave a new pore radius close to 4 nm. Kallala et al. [28] investigated the structures of the oxopolymers by SAXS. It was proposed that the growth of oxopolymers occurs through a two-stage growth process in which a few large polymers grow first and then densify through the capture of residual monomers. Kamiyama et al. [29] investigated the gelation process of Ti(IV)-isopropoxide solutions as a function of the reaction time, also using SAXS. By slowly adding water, the solution was kept transparent throughout the gelation. A fractal structure of the size of about 12 nm was observed. When the water was rapidly added, the solution became opaque before the gelation point. In this case the fractal structure of about 2.5 nm in size was measured.

### 3.2. Physical characterizations of nanosized TiO<sub>2</sub>

#### 3.2.1. High resolution electron microscopy and electron diffraction

The results obtained with two samples, S1 and S2, are given in Table 1. The HREM image and the corresponding ED pattern of sample S2 stabilized with HPC and

TABLE 1. Grain size determined by HREM, XRD, SAXS and Raman spectroscopy. Legend: A=anatase, B=brookite, R=rutile, d=dominant phase, NM=not measurable because of sharp diffraction lines.

Sample	Heat treatment (K)	Phase composition by XRD & ED	Grain size (nm)			
			HREM	XRD	SAXS	Raman
S1	423 573 913	A(d)+B	4.5 ± 2.0	6 ± 1		7.0
S1		A(d)+B		7 ± 2		8.1
S1		A(d)+B		9 ± 2		10.0
S1		R(d)+B		NM		
S1	1273	R	A:6.5 ± 2.0	NM		
S2	573 773	A(d)+B	5 ± 2	5 ± 1	4	6.6
S2		A(d)+B		7 ± 2		10.5
S2		A(d)+B		9 ± 3		12 ± 3

heated to 573 K are shown in Figs. 1a, b and d. These images reveal nanocrystalline grain sizes of 2 to 8 nm in diameter and pores sized from 1.5 to 10 nm. The distribution of grain sizes, as measured from HREM images, was fitted to the Gaussian curve (Fig. 1c), giving an average size of (5 ± 2) nm [15]. According to ED, this sample consisted of nanocrystalline and amorphous phases. Diffraction rings were ascribed to anatase and brookite. A magnified part of Fig. 1a is shown in Fig. 1d, revealing nanocrystalline grain sizes, pores, and amorphous regions.

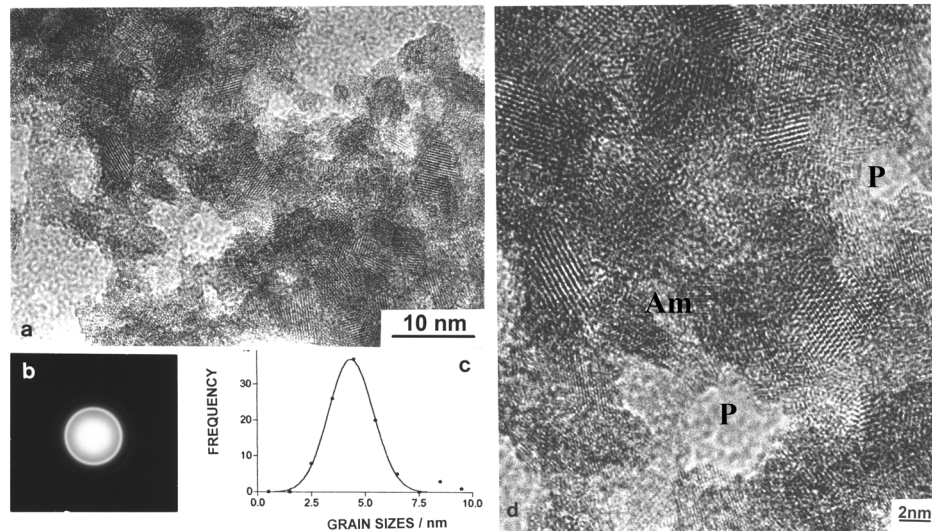


Fig. 1.  $\text{TiO}_2$  sample S2 (starting thin solid film heated up to (573 K): a) HREM image showing nanocrystalline grains of anatase and brookite, of size  $(5 \pm 2)$  nm, and pores of size from 1.5 to 10 nm; b) the corresponding ED pattern; c) the distribution of size of grains, measured by HREM, and fitted by the Gaussian curve; d) magnified part of HREM image a); the overlapped grains, pores (P) and regions of amorphous phase (Am).

The HREM image of the sample S2, heated to about 773 K, shown in Fig. 2a, gave the grain sizes from 7 to 12 nm, the average being  $(9 \pm 3)$  nm (statistical average of three images). The sizes of pores varied from 7 to 12 nm [15]. The corresponding ED pattern (inset in Fig. 2a) revealed nanocrystalline anatase and brookite. The HREM image, given in Fig. 2c, shows amorphous regions of HPC surrounding a brookite grain; its lattice planes (111), having a spacing of 0.346 nm, are clearly resolved. The role of organic polymer HPC is to prevent sintering of crystal grains during the heating; however, a slow increase of grain sizes is observed with an increase of the temperature.

The HREM images of sample S1, prepared without HPC [14,16,30] and heated to about 913 K, revealed crystal grains of rutile having sizes from 150 to 700 nm, and small grains of anatase.

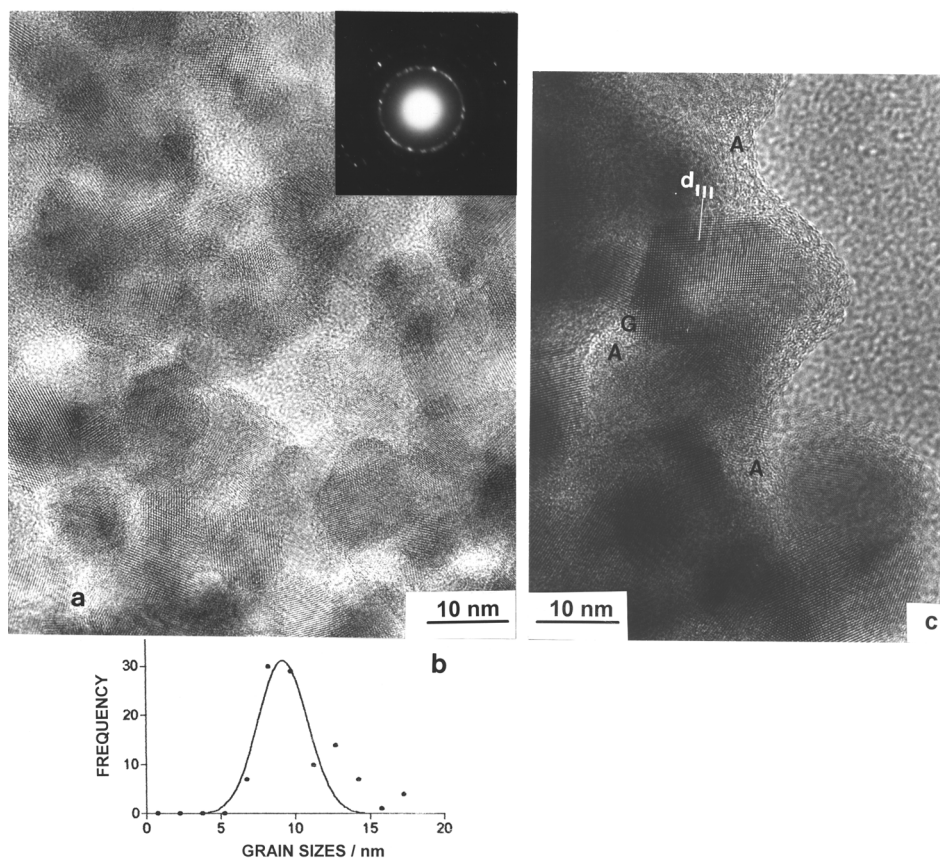


Fig. 2.  $\text{TiO}_2$  sample S2 (starting thin solid film heated up to 773 K): a) HREM image showing nanocrystalline grains of anatase and brookite, of size  $(9 \pm 3)$  nm; the corresponding ED pattern is shown in the inset; b) the distribution of grain (G) sizes, measured by HREM, and fitted by the Gaussian curve; c) HREM image showing a grain of brookite (B), surrounded with amorphous region A of HPC (Am); the lattice planes (111) having the spacing of 0.346 nm are shown in brookite grain.

### 3.2.2. X-ray diffraction

XRD powder patterns of the starting samples, S1 and S2, heated to different temperatures are shown in Fig. 3a and b. All starting samples and heated samples were identified as mixtures of anatase as the dominant phase, and brookite; this is in accordance with the results of ED. Both phases exhibited a pronounced diffraction

broadening, which decreased as the heat-treatment temperature increased. The crystallite



size of the samples were estimated using the well-known Scherrer equation:

$$D = \frac{0.9\lambda}{\beta \cos\theta}, \quad (3)$$

where  $\lambda$  is the X-ray wavelength,  $\theta$  the Bragg angle and  $\beta$  the pure full width of the diffraction line at one the half of the maximum intensity.

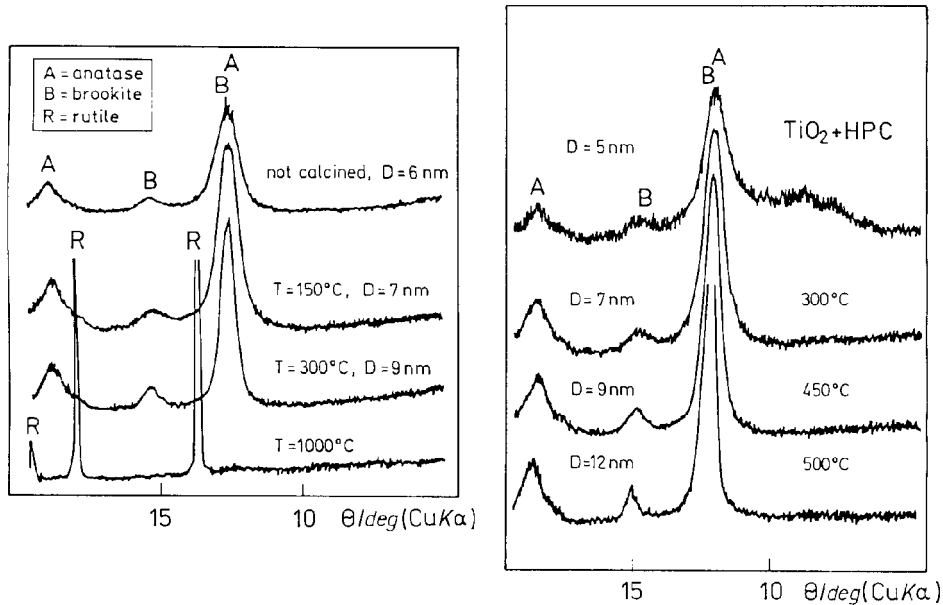


Fig. 3. X-ray powder diffraction patterns of samples S1 and S2, heated to different temperatures (A=anatase, B=brookite, R=rutile, D=estimated crystallite size).

The average crystallite size increased from 5 to 12 nm with an increase of temperature up to 773 K for the sample S2, and from 6 to 9 nm with an increase of temperature up to 573 K for the sample S1 (Table 1). However, the sample S1, heated up to about 1270 K, exhibited the well-crystallized rutile. XRD results are in agreement with those of HREM and ED.

### 3.2.3. Small-angle X-ray scattering

SAXS data for TiO<sub>2</sub> sample S2 on a glass substrate are shown in Fig. 4, together with the fitted curves in the Guinier plot. Small-angle X-ray scattering is caused because of the different electron density within the grains and in the surrounding material. The scattering at very small angles is of a Gaussian form, and the Guinier plot yields the grain sizes. The grain size estimated for the starting sample and the size found for the same sample heated to 773 K are given in Table 1.

### 3.2.4. Low-frequency Raman scattering

We analyzed low-frequency Raman modes at about  $20\text{ cm}^{-1}$  (Fig. 5) as a new method for the determination of grain sizes in nanosized  $\text{TiO}_2$  [14,17]. This method is based on the work of Duval et al. [31], originally applied to crystallized glasses. The maximum of the low-frequency Raman band is proportional to the inverse diameter of the spherical grains. The wave number  $\nu$  (in  $\text{cm}^{-1}$ ) of the lowest-energy spherical mode of a

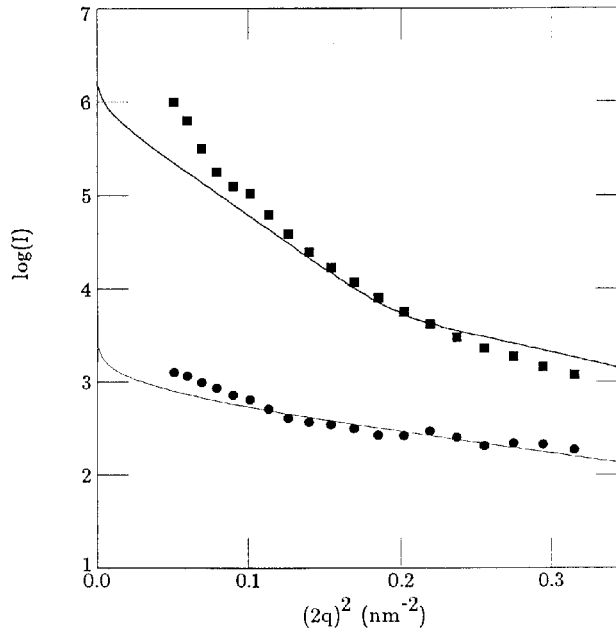


Fig. 4. SAXS data for the sample S2, not-heated (squares) and heated to 773 K (circles): Guinier plot relating  $\log I$  and  $(2q)^2$ , where  $I$  is the scattered intensity, and  $q$  the wave vector in  $\text{nm}^{-1}$ .

free grain, corresponding to the angular momentum  $l = 0$ , is given, according to Lamb [32] and Tamura et al. [33], as

$$\nu \approx \frac{0.7v_l}{dc}, \quad (4)$$

where  $v_l$  is the speed of longitudinal sound waves,  $c$  the velocity of light in vacuum and  $d$  the grain diameter. For the longitudinal velocity of the sound, the average value for rutile of  $v_l = 9022\text{ m/s}$  was used, assuming that the difference in the longitudinal velocity of sound in various  $\text{TiO}_2$  polymorphs is not large. The Raman spectra recorded were corrected for linear background and the Bose-Einstein factor.

The grain size of nanosized  $\text{TiO}_2$  determined by low-frequency Raman scattering, as presented in Table 1, is in good agreement with the results of other techniques (sections 3.2.1., 3.2.2. and 3.2.3.).

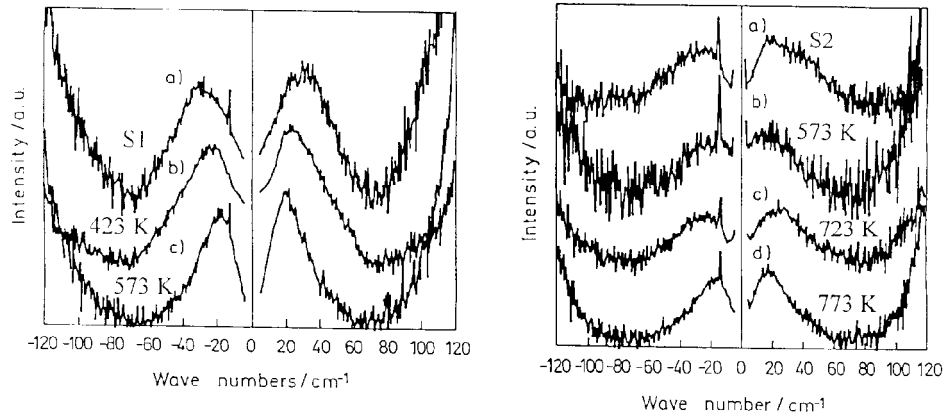


Fig. 5. Low-frequency Raman modes at about  $20 \text{ cm}^{-1}$  after baseline and temperature corrections. a)  $\text{TiO}_2$  sample S1 (starting sample) and samples heated to 423 and 573 K; b)  $\text{TiO}_2$  sample S2 (starting sample) and samples heated to 573, 723 and 773 K.

#### 4. Conclusion

Following the procedure by Grätzel and his research group, but using titanium dioxide films as photoanodes prepared by our original method, we have produced solar cells with better efficiencies than those using commercial P25  $\text{TiO}_2$  [34]. The hydrolysis of Ti(IV)-isopropoxide in isopropanol by the addition of water is a suitable chemical reaction for the production of nanosized  $\text{TiO}_2$ . The phase composition of the products of the aging of the  $\text{TiO}_2$  precursor depends on its colloidal state (polymer, sol, gel or precipitate). The hydrolysis catalysts, pH, temperature, and the presence of a complexing agent, are also factors which influence the sol-gel synthesis of  $\text{TiO}_2$ .

The experimental conditions for the synthesis of  $\text{TiO}_2$  with small grain sizes of 4 to 12 nm were defined using TEM, HREM, XRD, SAXS and Raman. The grain sizes depended on the modification of the general sol-gel procedure. It was found that the grain sizes gradually increased to 12 nm with an increase of the heating temperature up to 773 K. Electron diffraction and X-ray diffraction gave evidence of nanocrystalline anatase and brookite. The grain sizes of the anatase and brookite phases changed from  $(5 \pm 1)$  to  $(12 \pm 3)$  nm with an increase of temperature up to 773 K, as shown by XRD. The small grain size, high specific area, good porosity and desirable phase composition of nanosized  $\text{TiO}_2$  samples synthesized in our work, are properties ensuring good properties of this material in the tested dye-sensitized solar cells. It is suggested that the mixture of anatase and brookite played an important role in the construction of dye-sensitized solar cells, where  $\text{TiO}_2$  was used as a carrier for ruthenium-dye complex [34]. Grain sizes obtained using different methods are in good agreement [35]; however, when we compare these methods, it is important to keep in mind that grain size definition is specific for each method.

#### References

- 1) B. Vlahović and M. Peršin, *J. Phys. D: Appl. Phys.* **23** (1990) 1324;
- 2) A. Turković and V. Vraneša, *Int. J. Mater. Product Techn.* **47** (1992) 51. (This paper was presented at the first European East-West Symposium on Materials and Processes, 1990.);
- 3) A. Turković, M. Ivanda, A. Drašner, V. Vraneša and M. Peršin, *Thin Solid Films* **198** (1991) 199;
- 4) A. Turković and M. Ivanda, *Solid State Ionics* **50** (1992) 159;
- 5) A. Turković, M. Ivanda, J. Tudorić-Ghemo, N. Godinović and I. Sorić, *Oxygen Non-Stoichiometry in Thermally Annealed and Hydrogen Implanted TiO<sub>2</sub> Thin Films Observed by Raman Spectroscopy*, in *Non-Stoichiometry in Semiconductors*, Editors K. J. Bachmann, H.-L. Hwang, C. Schwab, Elsevier Sci. Publ. **A3** (1991) 307;
- 6) A. Turković, M. Ivanda, V. Vraneša and A. Drašner, *Vacuum* **43** (1992) 471;
- 7) A. Turković, D. Šokčević, M. Milun, T. Valla and J. Rukavina, *Fizika A* **2** (1993) 23;
- 8) A. Turković and D. Šokčević, *Appl. Surf. Sci.* **68** (1993) 477;
- 9) A. Turković, N. Radić and D. Šokčević, *Mater. Sci. Eng.* **B23** (1994) 41;
- 10) K. Zweibel, *Harnessing Solar Power; The Photovoltaic Challenge*, Plenum Press, New York, 1990;
- 11) B. O'Regan and M. Grätzel, *Nature* **353** (1991) 737;
- 12) M. K. Nazeeruddin, A. Kay, I. Rodicio, R. Humphry-Baker, E. Muller, P. Liska, N. Vlachopoulos and M. Grätzel, *J. Am. Chem. Soc.* **115** (1993) 6382;
- 13) M. Gotić, B. Gržeta, S. Musić, S. Popović, A. Tonejc, R. Trojko and A. Turković, *X-ray and Electron Diffraction, TEM, HREM and DTA of Nanosized TiO<sub>2</sub> as Photoanode for Dye-sensitized Solar Cell*, *Fourth Croatian-Slovenian Crystallographic Meeting*, Trakošćan, Croatia, Sept. 28 – 30, 1995, Book of Abstracts, p. 16;
- 14) M. Gotić, M. Ivanda, A. Sekulić, S. Musić, S. Popović, A. Turković and K. Furić, *Mater. Lett.* **28** (1996) 225;
- 15) A. M. Tonejc, M. Gotić, B. Gržeta, S. Musić, S. Popović, R. Trojko, A. Turković and I. Mužević, *Mater. Sci. Eng.* **B40** (1996) 177;
- 16) A. M. Tonejc, A. Turković, M. Gotić, S. Musić, M. Vuković, R. Trojko and A. Tonejc, *Mater. Lett.*, in press;
- 17) M. Gotić, M. Ivanda, S. Popović, S. Musić, A. Sekulić, A. Turković and K. Furić, *J. Raman. Spectr.*, in press;
- 18) S. Musić, M. Gotić, M. Ivanda, S. Popović, A. Turković, R. Trojko, A. Sekulić and K. Furić, *Mater. Sci. Eng. B*, in press;
- 19) D. Papoutsis and P. Lianos, *Langmuir* **11** (1995) 1;
- 20) P. Lianos and D. Papoutsis, *Progr. Colloid Polym. Sci.* **97** (1994) 240;
- 21) V. G. Courtecuisse, K. Chhor, J. F. Bocquet, C. Pommier, *Ind. & Eng. Chem. Res.* **35** (1996) 2539;
- 22) G. Dagan and M. Tomkiewicz, *J. Phys. Chem.* **97** (1993) 12651;
- 23) T. Nishide and F. Mizukami, *J. Ceram. Soc. Jpn.* **100** (1992) 1122;
- 24) V. J. Nagpal, R. M. Davis and S. B. Desu, *J. Mater. Res.* **12** (1995) 3068;
- 25) H. Asoka, *Mater. Lett.* **19** (1994) 207;
- 26) T. Lopez, E. Sanchez, P. Bosch, Y. Meas and R. Gomez, *Mater. Chem. Phys.* **32** (1992) 141;
- 27) A. Larbot, I. Laaziz, J. Marignan and J. F. Quinson, *J. Non-Crystall. Solids* **147&148** (1992) 157;

- 28) M. Kallala, C. Sanchez and B. Cabane, *Phy. Rev.* **E 48** (1993) 3692;
- 29) T. Kamiyama, N. Yoshida and K. Suzuki, *Bull. Inst. Chem., Res. Kyoto Univ.*, **72** (1994) 225;
- 30) A. M. Tonejc, A. Turković, M. Gotić, B. Gržeta, S. Musić, S. Popović and R. Trojko, *Int. Symp. on Metastable Mechanically Alloyed and Nanocrystalline Materials*, ISMANAM-96, Rome, Italy, May 20-24, 1996, P-D-5;
- 31) E. Duval, A. Boukenter and B. Champagnon, *Phys. Rev. Lett.* **56** (1986) 2052;
- 32) H. Lamb, *Proc. London Math. Soc.* **13** (1982) 187;
- 33) A. Tamura, K. Higeta and T. Ichinokawa, *J. Phys.* **C15** (1982) 4975;
- 34) A. Turković, H. Zorc, D. Kontrec and V. Vraneša, *Strojarstvo*, in press;
- 35) A. Turković, M. Ivanda, S. Popović, A. M. Tonejc, M. Gotić, P. Dubček and S. Musić, *J. Mol. Struct.*, in press.

#### STUDIJ NANOFAZNOG TiO<sub>2</sub> ELEKTRONSKOM MIKROSKOPIJOM, DIFRAKCIJOM X-ZRAČENJA I RAMANOVIM RASPRŠENJEM

Solarne ćelije senzitivirane bojom razlikuju se od klasičnih poluvodičkih uređaja u tome da imaju odvojenu funkciju apsorpcije svjetla od transporta nositelja naboja. Nov tip solarne ćelije osniva se na 10- $\mu$ m-debelom, optički prozirnom filmu titanovog dioksida (TiO<sub>2</sub>) čija su zrna veličine nekoliko nm. Oksidni film je prekriven monoslojem boje za prenošenje naboja kojom se izvodi senzitivacija filma za sakupljanje svjetla.

U ovom se radu istražuju mikrostrukturalna svojstva TiO<sub>2</sub> nanoveličine primjenom visokorezolucijske elektronske mikroskopije, elektronske difrakcije, difrakcije X-zračenja, raspršenjem rentgenskog zračenja pod malim kutom i Ramanovog raspršenja. U zrnima TiO<sub>2</sub> detektirani su anatas i brukit primjenom elektronske difrakcije i difrakcije X-zračenja. Veličina zrna anatasa i brukita su bile od (5  $\pm$  1) do (12  $\pm$  3) nm s odgovarajućim povećanjem temperature do 773 K, što je određeno difrakcijom X-zračenja. Prikazana je nova metoda određivanja veličine zrna TiO<sub>2</sub> nanoveličine primjenom niskofrekvencijskog Ramanovog raspršenja. Postignuto je dobro slaganje rezultata pri određivanju nanoveličine zrna TiO<sub>2</sub> navedenim instrumentalnim tehnikama.